ELSEVIER

Physica D 155 (2001) 112–131

PHYSICA D

www.elsevier.com/locate/physd

Traveling spike autosolitons in the Gray–Scott model

C.B. Muratov [a,*], V.V. Osipov [b]

[a] *Department of Mathematical Sciences, New Jersey Institute of Technology, University Heights, Newark, NJ 07102, USA*
[b] *CSIC, Laboratorio de Fisica de Sistemas Pequeños y Nanotecnologia, Calle Serrano 144, 28006 Madrid, Spain*

Received 31 July 2000; received in revised form 16 February 2001; accepted 9 March 2001

Communicated by C.K.R.T. Jones

Abstract

We developed singular perturbation techniques based on the strong separation of time and length scales to construct the solutions in the form of the traveling spike autosolitons (self-sustained solitary waves) in the Gray–Scott model of an autocatalytic reaction. We found that when the inhibitor diffusion is sufficiently slow, the ultrafast traveling spike autosolitons are realized in a wide range of parameters. When the diffusion of the inhibitor is sufficiently fast, the slower traveling spike autosolitons with the diffusion precursor are realized. We asymptotically calculated the main parameters such as speed and amplitude of these autosolitons as well as the regions of their existence in the Gray–Scott model. We also showed that in certain parameter regions the traveling spike autosolitons coexist with static.

Keywords: Pattern formation; Self-organization; Reaction–diffusion systems; Singular perturbation theory

1. Introduction

Self-organization and pattern formation in nonequilibrium systems are among the most fascinating phenomena in nonlinear physics [1–11]. Pattern formation is observed in various physical systems including fluids; gas and electron–hole plasmas; various semiconductor, superconductor and gas-discharge structures; some ferroelectric, magnetic and optical media; combustion systems (see, for example [5,9–14,53,54]), as well as in many chemical and biological systems (see, for example [1–7,15,55,56]).

Self-organization is often associated with the destabilization of the homogeneous state of the system [1,2,5,10,11]. At the same time, when the homogeneous state of the system is stable, one can excite large-amplitude patterns, including *autosolitons* (ASs) — self-sustained solitary inhomogeneous states, by applying a sufficiently strong stimulus [8–11,16–19,57–60]. Autosolitons are elementary objects in open dissipative systems away from equilibrium. They share the properties of both solitons and traveling waves (or autowaves, as they are also referred to [2,6]). They are similar to solitons since they are localized objects whose existence is due to the nonlinearities of the system. On the other hand, from the physical point of view they are essentially different from solitons in that they are *dissipative structures*, that is, they are self-sustained objects which form in strongly dissipative systems as a result of the balance between the dissipation and pumping of energy or matter. This is the reason why, in contrast to solitons, their properties are independent of the initial conditions and are determined primarily by the nonlinearities of the system [8–11].

* Corresponding author.
E-mail address: muratov@m.njit.edu (C.B. Muratov).

0167-2789/01/$ – see front matter
PII: S0167-2789(01)00259-7

A prototype model used to study pattern formation in nonequilibrium systems is a pair of reaction–diffusion equations of the activator–inhibitor type

$$\tau_\theta \frac{\partial \theta}{\partial t} = l^2 \Delta\theta - q(\theta, \eta, A), \tag{1}$$

$$\tau_\eta \frac{\partial \eta}{\partial t} = L^2 \Delta\eta - Q(\theta, \eta, A), \tag{2}$$

where θ is the activator, η the inhibitor, τ_θ, l and τ_η, L are the time and the length scales of the activator and the inhibitor, respectively; A is the control (bifurcation) parameter; q and Q are certain nonlinear functions representing the activation and the inhibition processes. Examples of these equations for various physical systems are given in [9–13,20] where the physical meaning of the variables θ and η and the nature of the activation and the inhibition processes are discussed. The well-known Brusselator [1] and the Gray–Scott [21] models of autocatalytic chemical reactions, the classical Gierer–Meinhardt model of morphogenesis [22], the FitzHugh–Nagumo [23,61] and the piecewise-linear Rinzel–Keller model [24,62] for the propagation of pulses in the nerve fibers are all special cases of Eqs. (1) and (2).

The fact that θ is the activator means that for certain parameters the uniform fluctuations of θ will grow when the value of η is fixed. From the mathematical point of view, this is given by the condition [9–11,18,60]

$$q_\theta < 0, \tag{3}$$

where $q_\theta = \partial q / \partial \theta$, for certain values of θ and η. On the other hand, the fact that η is the inhibitor means that its own fluctuations decay and that it damps the fluctuations of the activator. Mathematically, these conditions are expressed by [9–11,18,60]

$$Q_\eta > 0, \qquad q_\eta Q_\theta < 0 \tag{4}$$

for all values of θ and η, provided that the derivatives in Eq. (4) do not change sign.

Kerner and Osipov [8–11,16–18,20,57–60] showed that the properties of patterns and self-organization scenarios in systems described by Eqs. (1) and (2) are chiefly determined by the parameters $\epsilon \equiv l/L$ and $\alpha \equiv \tau_\theta / \tau_\eta$ and the shape of the nullcline of the equation for the activator, that is, the dependence $\eta(\theta)$ given by the equation $q(\theta, \eta, A) = 0$ for $A = \text{const}$. They demonstrated that depending on the shape of the activator nullcline the majority of systems can be divided into two fundamentally different classes: N-systems, for which the nullcline is N- or inverted N-shaped and, Λ- or V-systems, for which the nullcline is Λ- or V-shaped, respectively (see Fig. 1).

Most works devoted to the description of pattern formation on the basis of Eqs. (1) and (2) deal with N-systems. In N-systems the equation $q(\theta, \eta, A) = 0$ has three roots: θ_1, θ_2, and θ_3, for given values of A and η. The roots θ_1 and θ_3 correspond to the stable states and θ_2 corresponds to the unstable state in the system with $\eta = \text{const}$. It is easy to see that the FitzHugh–Nagumo and the piecewise-linear models belong to N-systems. For these models it was shown [24,25,62,63] that Eqs. (1) and (2) with $L = 0$ and

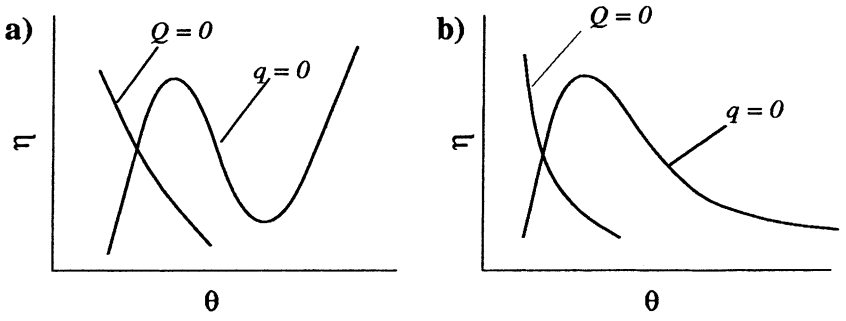

Fig. 1. Two qualitatively different types of the nullclines of Eqs. (1) and (2): N-systems (a) and Λ-systems (b).

$\alpha = \tau_\theta/\tau_\eta \ll 1$ have solutions in the form of the traveling waves (also called autowaves [2,6], or traveling ASs [8–11]). For $\alpha \ll 1$ these ASs consist of fronts and backs in which the activator varies sharply while the inhibitor remains almost constant, separated by regions in which both the inhibitor and the activator vary smoothly. It was found that in N systems the speed of these ASs cannot exceed values of order l/τ_θ [9,11,18,24,25,60,62,63]. In [16–19,57–60] it was shown that in another limit $L \gg l$ (or, more precisely, when $\epsilon = l/L \ll 1$ and $\alpha \gtrsim 1$) N-systems admit solutions in the form of the stable static patterns including ASs (see also [9–11]). Furthermore, it was shown that in N-systems with $\epsilon \ll 1$ and $\alpha \ll 1$ one can excite static, pulsating, and traveling patterns [8–11,18,20,26–31,60,64–67].

On the other hand, there are many physical, chemical and biological systems for which the activator nullcline is Λ- or V-shaped (Fig. 1(b)). In this case the equation $q(\theta, \eta, A) = 0$ for given A and η has only two roots: θ_1 corresponding to the stable state, and θ_2 corresponding to the unstable state in the system with $\eta = \text{const}$ [9–11,16,57,58]. Among Λ-systems are many semiconductor and gas-discharge structures, electron–hole and gas plasmas, radiation heated gas mixtures (see, for example [9–12,16,20,57,58]). It is not difficult to see that the Brusselator and the Gray–Scott models are Λ-systems, and the Gierer–Meinhardt model is a V-system.

Kerner and Osipov [9,11,16,32,33,57,58] qualitatively showed that in Λ-systems the so-called spike ASs and more complex spike patterns can be excited. They analyzed the static spike ASs and strata in the Brusselator, the Gierer–Meinhardt model, and the electron–hole plasma [16,32,57,58]. They found that when $\epsilon \ll 1$ and $\alpha \gtrsim 1$, the one-dimensional static spike AS can have small size of order l and huge amplitude which goes to infinity as $\epsilon \to 0$. Dubitskii et al. [11,32] formulated the asymptotic procedure for finding the stationary solutions in Λ-systems for sufficiently small ϵ. In [34] we showed that in another limiting case $\alpha \ll 1$ and $\epsilon \gg 1$ one can excite the one-dimensional traveling spike AS which also has small size and whose amplitude goes to infinity as $\alpha \to 0$. We also showed that, in contrast to the traveling patterns in N-systems, the velocity of this one-dimensional traveling spike AS can have huge values ($c \gg l/\tau_\theta$) and that the inhibitor distribution varies stepwise in the front of the spike. Thus, one can see that the properties of the spike patterns forming in Λ-systems differ fundamentally from those of the domain patterns forming in N-systems [35,68–70]. At the same time, spike patterns including the spike ASs are observed experimentally in the nerve tissue [36], chemical reactions [5,37], electron–hole plasma [38,71], gas-discharge structures [39,72], as well as numerically in the simulations of the Brusselator, the Gierer–Meinhardt, and the Gray–Scott models [1,15,22,40,41,55,56,73].

Let us emphasize that ϵ or α are the natural small parameters in the systems under consideration. Their relative smallness is in fact a necessary condition for the feasibility of any patterns [9–11]. Indeed, if the inverse were true, that is, if both the characteristic time and length scales of the variation of the inhibitor were much smaller than those of the activator, the inhibitor would easily damp all the deviations of the activator from the homogeneous steady state, making the formation of any kinds of persistent patterns impossible. On the other hand, the fact that we must have either $\epsilon \lesssim 1$ or $\alpha \lesssim 1$ for the patterns to be feasible implies that it is advantageous to consider the asymptotic limits $\epsilon \ll 1$ and/or $\alpha \ll 1$, which should result in a significant simplification of the original highly nonlinear problem. Note that this kind of approach has been successfully applied to a variety of pattern formation problems (see, for example [42,74–76]).

This paper is one in a series of papers devoted to an asymptotic study of the spike ASs in the Gray–Scott model of an autocatalytic chemical reaction. We chose the Gray–Scott model because it has an advantage of relatively simple nonlinearities, which in many cases allow to obtain explicit analytic results. Also, because of this one can expect a certain degree of universality of pattern formation exhibited by it. In this paper we concentrate on the traveling spike ASs, so we will study the one-dimensional Gray–Scott model with $\alpha \ll 1$ and different values of ϵ. We will develop formal asymptotic methods for the description of these patterns and study their major properties.

The outline of our paper is as follows. In Section 2 we introduce the model we will study, in Section 3 we asymptotically construct the solutions in the form of two types of traveling spike ASs, in Section 4 we compare our results with the numerical simulations, and in Section 5 we draw conclusions.

2. The model

The Gray–Scott model describes the kinetics of a simple autocatalytic reaction in an unstirred flow reactor. The reactor is a narrow space between two porous walls. Substance Y whose concentration is kept fixed outside of the reactor is supplied through the walls into the reactor with the rate k_0 and the products of the reaction are removed from the reactor with the same rate. Inside the reactor Y undergoes the reaction involving an intermediate species X:

$$2X + Y \xrightarrow{k_1} 3X, \tag{5}$$

$$X \xrightarrow{k_2} \text{inert}. \tag{6}$$

The first reaction is a cubic autocatalytic reaction resulting in the self-production of species X; therefore, X is the activator species. On the other hand, the production of X is controlled by species Y, so Y is the inhibitor species. The equations of chemical kinetics which describe the spatiotemporal variations of the concentrations of X and Y in the reactor and take into account the supply and the removal of the substances through the porous walls take the following form [21]:

$$\frac{\partial X}{\partial t} = -(k_0 + k_2)X + k_1 X^2 Y + D_X \Delta X, \tag{7}$$

$$\frac{\partial Y}{\partial t} = k_0(Y_0 - Y) - k_1 X^2 Y + D_Y \Delta Y, \tag{8}$$

where now X and Y are the concentrations of the activator and the inhibitor species, respectively, Y_0 is the concentration of Y in the reservoir, Δ the two-dimensional Laplacian, and D_X and D_Y are the diffusion coefficients of X and Y.

In order to be able to understand various pattern formation phenomena in a system of this kind, it is crucial to introduce the variables and the time and length scales that truly represent the physical processes acting in the system. The first and the most important is the choice of the characteristic time scales. These are primarily dictated by the time constants of the dissipation processes. For Y this is the supply and the removal with the rate k_0, whereas for X this is the removal from the system and the decay via the second reaction with the total rate $k_0 + k_2$. The natural way to introduce the dimensionless inhibitor concentration is to scale it with Y_0. Since we want to fix the time scale of the variation of the inhibitor (with the fixed activator), we will rescale X in such a way that the reaction term in Eq. (8) will generate the same time scale as the dissipative term. This leads to the following dimensionless quantities:

$$\theta = \frac{X}{X_0}, \qquad \eta = \frac{Y}{Y_0}, \quad X_0 = \left(\frac{k_0}{k_1}\right)^{1/2}. \tag{9}$$

The characteristic time and length scales for these quantities are

$$\tau_\theta = (k_0 + k_2)^{-1}, \qquad \tau_\eta = k_0^{-1}, \tag{10}$$

$$l = (D_X \tau_\theta)^{1/2}, \qquad L = (D_Y \tau_\eta)^{1/2}. \tag{11}$$

Naturally, one should require positivity of θ and η.

If we now write Eqs. (7) and (8) in terms of the dimensionless quantities θ and η, we will arrive at the following set of equations:

$$\tau_\theta \frac{\partial \theta}{\partial t} = l^2 \Delta\theta + A\theta^2\eta - \theta, \tag{12}$$

$$\tau_\eta \frac{\partial \eta}{\partial t} = L^2 \Delta\eta - \theta^2\eta + 1 - \eta \tag{13}$$

with the dimensionless parameters $\epsilon = l/L$, $\alpha = \tau_\theta/\tau_\eta$ and A:

$$\epsilon = \left(\frac{k_0 D_X}{(k_0 + k_2) D_Y}\right)^{1/2},$$
$$\alpha = \frac{k_0}{k_0 + k_2},$$
$$A = \frac{Y_0 k_0^{1/2} k_1^{1/2}}{k_0 + k_2}. \tag{14}$$

Note that in the literature the Gray–Scott model is often written in terms of semi-dimensionless parameters

A, B, D, which can be related to our parameters ϵ, α and A by noticing that $A = k_0, B = k_0 + k_2$, and $D = D_X$, when $Y_0 = D_Y = 1$.

One can see from Eqs. (12) and (13) that τ_θ and τ_η are in fact the characteristic time scales, and l and L the characteristic length scales of the variation of small deviations of θ and η from the stationary homogeneous state $\theta = \theta_\mathrm{h}$ and $\eta = \eta_\mathrm{h}$:

$$\theta_\mathrm{h} = 0, \qquad \eta_\mathrm{h} = 1. \tag{15}$$

As can be seen from Eq. (12), the parameter A is the dimensionless strength of the activation process, that is, it describes the degree of deviation of the system from thermal equilibrium. With all this, Eqs. (12) and (13) are reduced to the form of Eqs. (1) and (2). Notice that the system given by Eqs. (12) and (13) is indeed a system of the activator–inhibitor type: the condition in Eq. (3) is satisfied for $\theta > \frac{1}{2}A\eta$, and the conditions in Eq. (4) are satisfied with $q_\eta < 0$ and $Q_\theta > 0$ for all $\theta > 0$ and $\eta > 0$.

The nullclines of Eqs. (12) and (13) are shown in Fig. 2. From this figure one can see that the nullcline of the equation for the activator has degenerate Λ-form. It consists of two separate branches: $\theta = 0$ and $\theta = 1/A\eta$. Note that adding an extra small constant term in the right-hand side of Eq. (19) (which physically would correspond to some finite concentration of substance X in the reservoir), one can remove this degeneracy of the nullcline and make the nullcline truly Λ-shaped.

One can easily check that for $0 < A < 2$ there is only one stationary homogeneous state given by Eq. (15), whereas for $A > 2$ two extra stationary homogeneous states exist:

$$\theta_{\mathrm{h}2,3} = \frac{A \mp \sqrt{A^2 - 4}}{2}, \qquad \eta_{\mathrm{h}2,3} = \frac{A \pm \sqrt{A^2 - 4}}{2A}. \tag{16}$$

The stability analysis of these homogeneous states shows that for $\epsilon \ll 1$ or $\alpha \ll 1$ the homogeneous state $\theta = \theta_{\mathrm{h}2}$, $\eta = \eta_{\mathrm{h}2}$ is always unstable. For $\epsilon \ll 1$ the homogeneous state $\theta = \theta_{\mathrm{h}3}$, $\eta = \eta_{\mathrm{h}3}$ is unstable with respect to the Turing instability if $A < 0.41\epsilon^{-1}$. For $\alpha \ll 1$ it is unstable with respect to the homogeneous oscillations (Hopf bifurcation) if $0.41\alpha^{-1/2} < A < \alpha^{-1/2}$, or it is an unstable node if $A < 0.41\alpha^{-1/2}$. On the other hand, the homogeneous state $\theta = \theta_\mathrm{h}$, $\eta = \eta_\mathrm{h}$ is stable for all values of the system's parameters. The latter is simple to understand; in order for the reaction to begin there has to be at least some amount of the activator put in at the start. Equivalently, the fact that the homogeneous state in Eq. (15) is stable for all values of the parameter A (for an arbitrary deviation from thermal equilibrium) is the consequence of the degeneracy of the nullcline of Eq. (12). Thus, self-organization associated with the Turing instability of the homogeneous state $\theta_\mathrm{h} = 0$ and $\eta_\mathrm{h} = 1$ is not realized in the Gray–Scott model. In such a stable homogeneous system any inhomogeneous pattern, including ASs, can only be excited by a sufficiently strong localized stimulus. In turn, self-organization will occur

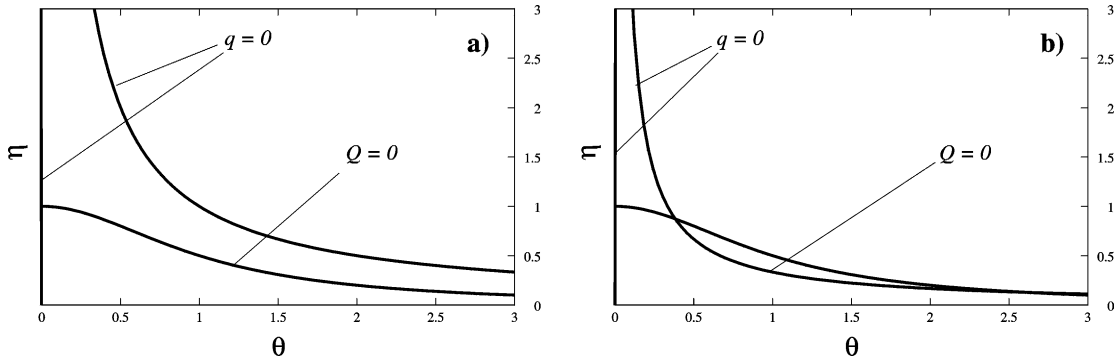

Fig. 2. The nullclines of Eqs. (12) and (13) for $A = 1$ (a) and $A = 3$ (b).

as a result of the instabilities of the large-amplitude patterns already present in the system.

Note that in the opposite case $\epsilon \gg 1$ and $\alpha \gg 1$ the dynamics of the system becomes dramatically simpler. Indeed, if we set both L and τ_η to zero, from Eq. (13) we get a local relationship $\eta = 1/(1+\theta^2)$. Substituting this back to Eq. (12), we obtain

$$\tau_\theta \frac{\partial \theta}{\partial t} = l^2 \Delta\theta + \frac{A\theta^2}{1+\theta^2} - \theta. \tag{17}$$

This equation possesses a simple variational structure

$$\tau_\theta \frac{\partial \theta}{\partial t} = -\frac{\delta \mathcal{F}}{\delta \theta},$$
$$\mathcal{F} = \int \mathrm{d}^d x \left(\frac{l^2 (\nabla\theta)^2}{2} - A\theta + A \arctan\theta + \frac{\theta^2}{2} \right). \tag{18}$$

For $A < 2$ the functional $\mathcal{F}$ has a unique global minimum at $\theta = \theta_\mathrm{h} = 0$, so any initial condition will decay to the homogeneous state θ_h. For $A > 2$ there are two stable homogeneous states $\theta = \theta_\mathrm{h}$ and $\theta = \theta_{\mathrm{h}3}$ (see above), so it is possible to have the waves of switching from one homogeneous state to the other [5]. It is easily checked that for $2 < A < 2.18$ the dominant homogeneous state is θ_h, while for $A > 2.18$ the dominant homogeneous state is $\theta_{\mathrm{h}3}$. Let us also mention the work of Hale et al. [43] for the case of $\alpha \simeq 1$ and $\epsilon \simeq 1$ (see also the remark in the conclusion of [47]).

In the case of $\alpha \ll 1$ it is convenient to scale length and time with l and τ_θ, respectively. In these units Eqs. (12) and (13) restricted to one dimension will take the following form:

$$\theta_t = \theta_{xx} + A\theta^2\eta - \theta, \tag{19}$$

$$\alpha^{-1}\eta_t = \epsilon^{-2}\eta_{xx} - \theta^2\eta + 1 - \eta. \tag{20}$$

We will assume that the problem is defined on the infinite domain with the boundary conditions,

$$\theta(\pm\infty) = \theta_\mathrm{h}, \qquad \eta(\pm\infty) = \eta_\mathrm{h}. \tag{21}$$

Notice that the kinetic model used to arrive at Eqs. (19) and (20) imposes a restriction $\alpha \leq 1$ (see Eq. (10)). For the sake of generality, in the following we will allow α to take on arbitrary values.

3. Traveling spike autosolitons

According to the general qualitative theory of ASs, for $\alpha = \tau_\theta/\tau_\eta \ll 1$ and ϵ sufficiently large, Eqs. (19) and (20) should have solutions that propagate with a constant speed without decay — traveling ASs [9–11]. As we will show below, in the Gray–Scott model traveling ASs are realized for sufficiently small α and have the shape of narrow spikes of high amplitude which strongly depends on α.

The equations describing an AS traveling with constant speed c along the x-axis take the form,

$$\frac{\mathrm{d}^2\theta}{\mathrm{d}z^2} + c\frac{\mathrm{d}\theta}{\mathrm{d}z} + A\theta^2\eta - \theta = 0, \tag{22}$$

$$\epsilon^{-2}\frac{\mathrm{d}^2\eta}{\mathrm{d}z^2} + \alpha^{-1}c\frac{\mathrm{d}\eta}{\mathrm{d}z} - \theta^2\eta + 1 - \eta = 0, \tag{23}$$

where we introduced a self-similar variable $z = x - ct$. The solution with $c > 0$ travels from left to right. The boundary conditions for these equations are given by Eq. (21).

3.1. Nondiffusive inhibitor: $\epsilon \gg \alpha^{1/2}$

There are two qualitatively different types of traveling spike ASs in the Gray–Scott model. First we consider the ultrafast traveling spike AS, which is realized when the inhibitor does not diffuse, that is, when $L = 0$ (or $\epsilon = \infty$). Such an AS was discovered by us in a similar reaction–diffusion model (the Brusselator) [34]. A remarkable property of this AS is that it has the shape of a narrow spike whose velocity $c \sim A\alpha^{-1/2}$ is much higher than the characteristic speed l/τ_θ (which in these units is of order 1) determined by the physical parameters of the problem, and whose amplitude goes to infinity as $\alpha \to 0$.

3.1.1. Case $\alpha^{1/2} \ll A \ll \alpha^{-1/2}$: ultrafast traveling spike autosoliton

If we assume that $\theta \gg 1$, we can drop the last term from Eq. (22) and neglect the last two terms in Eq. (23) (with the term involving the second derivative of η dropped in the limit of large ϵ) in the front of the spike where $\eta \sim \eta_\mathrm{h} = 1$. If we then multiply the latter

equation by A and add it to the former equation, we will get

$$\frac{\mathrm{d}^2\theta}{\mathrm{d}z^2} + c\frac{\mathrm{d}\theta}{\mathrm{d}z} + A\alpha^{-1}c\frac{\mathrm{d}\eta}{\mathrm{d}z} = 0. \tag{24}$$

This equation can be straightforwardly integrated. If we introduce the variables

$$\tilde{\theta} = \alpha A^{-1}\theta, \qquad \tilde{c} = \alpha^{1/2}A^{-1}c, \qquad \xi = A\alpha^{-1/2}z, \tag{25}$$

we can write the solution for η as

$$\eta = 1 - \tilde{\theta} - \frac{1}{\tilde{c}}\frac{\mathrm{d}\tilde{\theta}}{\mathrm{d}\xi}, \tag{26}$$

where we took into account the boundary condition $\tilde{\theta}(+\infty) = \tilde{\theta}_\xi(+\infty) = 0$, $\eta(+\infty) = 1$. Substituting this expression back to Eq. (22) (with the last term dropped), we arrive at the following equation:

$$\frac{\mathrm{d}^2\tilde{\theta}}{\mathrm{d}\xi^2} + \frac{\mathrm{d}\tilde{\theta}}{\mathrm{d}\xi}\left(\tilde{c} - \frac{1}{\tilde{c}}\tilde{\theta}^2\right) + \tilde{\theta}^2 - \tilde{\theta}^3 = 0. \tag{27}$$

One can see that in Eq. (27) all the α- and A-dependence is absent, so Eq. (25) (with all the tilde quantities of order 1) in fact determines the scaling of the main parameters of the traveling spike AS for $\alpha \ll 1$. As was expected, the AS will have the speed which diverges as $\alpha \to 0$. Also, note that the width of the front of the AS, which is of order $\alpha^{1/2}A^{-1}$ goes to zero as $\alpha \to 0$. Thus, the distributions of θ and η in the front of the ultrafast traveling spike AS will be given by the "supersharp" distributions (in the sense that their characteristic length scale is much smaller than 1) described by Eqs. (26) and (27).

Let us take a closer look at Eq. (27). This equation has the form of an equation of motion for a particle with the coordinate $\tilde{\theta}$ and time ξ in the potential $U = \frac{1}{3}\tilde{\theta}^3 - \frac{1}{4}\tilde{\theta}^4$ with the nonlinear friction with the coefficient $\tilde{c} - \tilde{\theta}^2/\tilde{c}$. Since the derivative of the friction coefficient is positive for all $\tilde{c}$, the friction increases as $\tilde{c}$ grows, so there are no special features associated with its nonlinearity. For $\tilde{\theta} > 0$ the potential U has a maximum at $\tilde{\theta} = 1$ and a minimum at an inflection point $\tilde{\theta} = 0$. The supersharp distribution of θ will therefore be the heteroclinic trajectory going from $\tilde{\theta} = 1$ to $\tilde{\theta} = 0$.

It is clear that if the friction is not strong enough, the particle starting from $\tilde{\theta} = 1$ will miss the point $\tilde{\theta} = 0$ and go to minus infinity, so we must have $\tilde{c} \geq \tilde{c}^*$, where $\tilde{c}^*$ is some positive constant of order 1. On the other hand, it is clear that when $\tilde{c} > \tilde{c}^*$, the particle will always get from $\tilde{\theta} = 1$ to $\tilde{\theta} = 0$, so in fact there is a continuous family of such solutions. Thus, we have a multiplicity of the front solutions and, therefore, a selection problem [5]. To answer the question about the front selection, we need to consider higher-order corrections to the solution of Eq. (27) coming from Eqs. (22) and (23). According to these equations, for small $\tilde{\theta}$ the next order correction will amount to adding the term $-\alpha A^{-2}\tilde{\theta}$ to Eq. (27). In this situation the potential U will actually have a maximum at $\tilde{\theta} = 0$ and a minimum at $\tilde{\theta}_{\min} \sim \alpha A^{-2}$, so only the trajectory with the minimum velocity $\tilde{c}$ will reach $\tilde{\theta} = 0$, whereas all other trajectories will be stuck at $\tilde{\theta} = \tilde{\theta}_{\min}$. Thus, we can conclude that in the limit $\alpha \to 0$ the selected front solution in our problem has the velocity $\tilde{c} = \tilde{c}^*$. The numerical solution of Eq. (27) shows that the value of $\tilde{c}^*$ is $\tilde{c}^* = 0.86$. The numerical simulations of Eqs. (12) and (13) confirm these conclusions. The main parameters of the traveling spike AS, therefore, are

$$\theta_{\max} = A\alpha^{-1}, \qquad c = 0.86A\alpha^{-1/2}. \tag{28}$$

Note that the numerical solution of Eq. (27) in the form of the supersharp front differs from $\tilde{\theta}_{\mathrm{ssh}} = \frac{1}{2}[1 - \tanh(0.50\xi)]$ by less than 1%. Also note that the results given by Eq. (28) precisely coincide with those obtained by us for the Brusselator [34]. This is due to the fact that the supersharp distributions in these two models are described by the same equations.

In the back of the supersharp front the value of $\tilde{\theta}$ goes exponentially to 1, and η goes exponentially to 0 (see Eq. (26)). Note, however, that in writing the equations describing the supersharp distributions we neglected the last two terms in Eq. (23). When the value of η decreases, at $\eta \sim \alpha^2A^{-2}$ the term $\theta^2\eta$ becomes of order 1, and the equations for the supersharp distributions cease to be valid. This will happen at a distance of order $\alpha^{1/2}A^{-1}\ln A\alpha^{-1}$ behind the location of the supersharp front. We can therefore call the region of this size right after the front where η

exponentially decays to some value $\eta_{\min}$ the secondary region of the supersharp distributions. Since the width of this region is still much smaller than 1, we can assume that $\theta = \theta_{\max}$ there. Then, the distribution of η in the secondary region of the supersharp distributions is given by Eq. (23) in which we should drop the last term, since $\eta \ll 1$ there. We obtain

$$\eta_{\mathrm{ssh2}} = \alpha^2 A^{-2} + C\,\mathrm{e}^{\xi/\tilde{c}}, \tag{29}$$

where the constant C should be determined by matching to the asymptotics of the supersharp distribution of η at $\xi \to -\infty$ (this requires an explicit knowledge of the solution in the supersharp region). As can be seen from this equation, we have $\eta_{\min} = \alpha^2 A^{-2}$.

As z passes the secondary region of the supersharp distributions, $\theta^2\eta$ becomes of order 1, and therefore can be dropped from Eq. (22). Then the activator and the inhibitor become decoupled, so the characteristic length scale of the variation of θ significantly increases. According to Eq. (22), for $c \gg 1$ the characteristic length scale of the decay of θ behind the supersharp front is of order $c \sim A\alpha^{-1/2}$, which is still much smaller than the length scale of the variation of η behind the spike (the refractory region), which is of order $\alpha^{-1}c$ (see below). This means that after the secondary region of the supersharp distributions we should find the region of the sharp distributions. According to Eq. (22) with the terms $\mathrm{d}^2\theta/\mathrm{d}z^2$ and $A\theta^2\eta$ dropped, the solution for θ in this region will be

$$\theta_{\mathrm{sh}}(z) = \alpha^{-1} A\,\mathrm{e}^{z/c}, \tag{30}$$

where we chose the position of the supersharp front to be at $z = 0$ (with the accuracy of α). This expression for θ_{sh} can be substituted back into Eq. (23) to calculate η_{sh}. The analysis of this equation then shows that one can neglect both $\alpha^{-1}c(\mathrm{d}\eta/\mathrm{d}z)$ and $-\eta$ in the region of the sharp distributions, so η_{sh} and θ_{sh} are related locally. The resulting expression for the sharp distribution of η takes the following form:

$$\eta_{\mathrm{sh1}} = \alpha^2 A^{-2}\,\mathrm{e}^{-2z/c}. \tag{31}$$

As will be shown in the next paragraph, this equation is in fact valid only in the part of the sharp distributions region, so we will call it the primary sharp distribution of η.

According to Eq. (31), the value of η exponentially grows behind the region of the sharp distributions, so at some distance of order $\alpha^{-1/2}A\ln\alpha^{-1}A^2$ one can no longer neglect the term $\alpha^{-1}c\,\mathrm{d}\eta/\mathrm{d}z$ in Eq. (23). If we take this derivative into account, we can solve Eq. (23), provided that θ is still given by Eq. (30). The solution will have the following form:

$$\eta_{\mathrm{sh2}}(z) = \tfrac{1}{2}\alpha\Gamma(0, \mathrm{e}^{(2/c)(z-z_0)})\,\mathrm{e}^{\mathrm{e}^{(2/c)(z-z_0)}},$$
$$z_0 = \tfrac{1}{2}c\ln 2\alpha A^{-2}, \tag{32}$$

where $\Gamma(a, x)$ is the incomplete gamma function. In writing the last equation we matched this solution with the one from Eq. (31) at large $z - z_0$. We will call this distribution of η the secondary sharp distribution.

For yet more negative values of z the distribution of η approaches $\eta \simeq -\alpha c^{-1} z$ (see Eq. (32)), so the characteristic length scale of the variation of η becomes of order $\alpha^{-1}c \gg c$. This means that we enter the refractory tail of the AS where η relaxes to η_{h}, that is, the region of the smooth distributions. For these values of z the distribution of θ already relaxed to zero, so Eq. (23) can be easily solved. To do that we should recall that up to $c \ll \alpha^{-1}c$ the region of the sharp distributions is located at $z = 0$, and to the leading order in α we have $\eta(0) = 0$. This immediately gives us the solution for η in the region of the smooth distributions

$$\eta_{\mathrm{sm}} = 1 - \mathrm{e}^{\alpha z/c}. \tag{33}$$

The entire solution in the form of the ultrafast traveling spike AS is presented in Fig. 3. This figure actually shows the result of the numerical simulations of Eqs. (19) and (20) with $\alpha = 10^{-3}$ and $A = 1$. One can see an excellent agreement of this solution with the distributions obtained above.

Thus, we introduced an asymptotic procedure for constructing the solution in the form of the traveling spike AS in the Gray–Scott model in the limit $\alpha \to 0$. This solution is considerably different from the solutions in the form of the traveling ASs in N-systems (see Section 1). In N-systems the speed and the distribution of θ in the AS front are determined only by the equation for the activator with $\eta = \eta_{\mathrm{h}}$ in the limit $\alpha \to 0$, so the speed of the AS cannot exceed the value of order 1 [9,11,24,25,62,63]. The distribution of θ in such

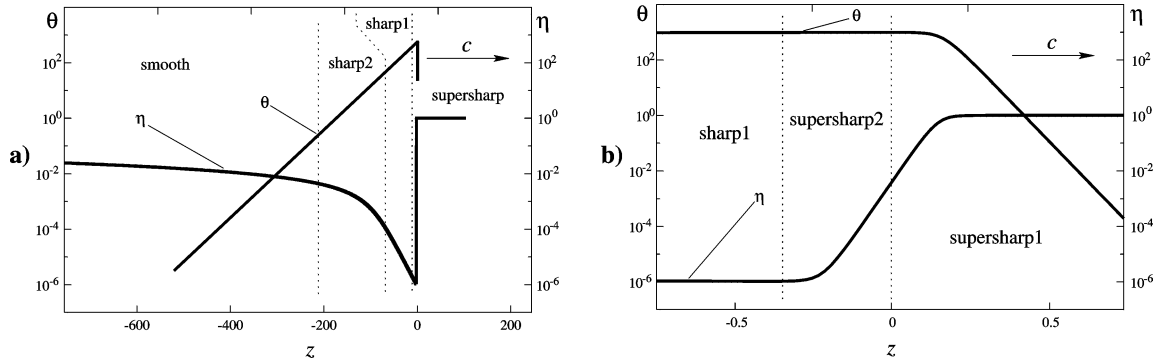

Fig. 3. Distributions of θ and η in the ultrafast traveling spike AS: (a) the back of the AS; (b) the front of the AS. Results of the numerical solution of Eqs. (19) and (20) with $\epsilon = \infty$, $\alpha = 10^{-3}$, and $A = 1$. Length is measured in the units of l.

an AS can be separated into two regions: the region of the sharp distributions, which corresponds to the moving domain wall whose characteristic size is of order 1, and the region of the smooth distributions, where the distribution of θ is slaved by the distribution of η which varies on the length scale of α^{-1} [11,25,63]. In other words, in the limit $\alpha \to 0$ there is only one boundary layer in the solution for θ (within a single domain wall) and no singularities in the solution for η. In contrast, in the Gray–Scott model the speed and the amplitude of the ultrafast traveling spike AS become singular in the limit $\alpha \to 0$. Moreover, there are *three* regions with different behaviors for θ in the ultrafast traveling AS: the region of the supersharp distributions, where θ varies on the length scale of $\alpha^{1/2}$, the region of the sharp distributions, in which the characteristic length scale of θ is $\alpha^{-1/2}$, and the region of the smooth distributions, where $\theta = 0$. The latter happens to be a specific property of the Gray–Scott model, in more general models the distribution of θ is slaved by the distribution of η in the smooth distributions and thus has the characteristic length scale of its variation of order $\alpha^{-1}c$ [34]. Moreover, the distribution of η can be separated into *five* regions where the asymptotic behavior of η is different. In other words, the solution in the form of the ultrafast traveling spike AS contains four boundary layers in the limit $\alpha \to 0$.

3.1.2. Case $A \sim \alpha^{1/2}$: disappearance of solution

According to the procedure presented above, the main parameters of the AS, such as the amplitude and the velocity are determined solely by the supersharp distributions of θ and η. However, according to Eq. (28), when A becomes of order $\alpha^{1/2}$, the velocity of the AS becomes of order 1, so the separation of the distributions of θ and η into the supersharp and the sharp distributions in the spike becomes invalid. For these values of A the treatment of the spike region has to be modified. Note that according to Eq. (28) we still have $\theta_{\max} \sim \alpha^{-1/2} \gg 1$ for $A \sim \alpha^{1/2}$. Let us introduce the following variables:

$$\tilde{\theta} = \alpha^{1/2}\theta, \qquad \tilde{\eta} = \eta, \qquad \tilde{A} = \alpha^{-1/2}A. \tag{34}$$

In these variables we can write Eqs. (22) and (23) as

$$\tilde{\theta}_{zz} + c\tilde{\theta}_z + \tilde{A}\tilde{\theta}^2\tilde{\eta} - \tilde{\theta} = 0, \tag{35}$$

$$c\tilde{\eta}_z - \tilde{\theta}^2\tilde{\eta} = 0, \tag{36}$$

where we neglected the last two terms in Eq. (23). These equations with the boundary conditions $\tilde{\theta}(\pm\infty) = 0$ and $\tilde{\eta}(+\infty) = 1$ can be solved numerically. Fig. 4(a) shows the solution of these equations for a particular value of $\tilde{A}$. One can see that the distribution of $\tilde{\theta}$ has the form of an asymmetric spike, while the distribution of $\tilde{\eta}$ goes from $\tilde{\eta} = 1$ at plus infinity to $\tilde{\eta} = \eta_{\min}$ at minus infinity. The numerical solution of Eqs. (35) and (36) shows that the traveling solution exists only for $\tilde{A} > \tilde{A}_{bT} = 3.76$. The numerical solution also shows that for $\tilde{A} > \tilde{A}_{bT}$ we have $\tilde{\eta}_{\min} < 0.05$, which decreases with the increase of $\tilde{A}$, so with good accuracy we can assume that $\eta_{\min} = 0$. Fig. 4(b) shows the dependence $c(\tilde{A})$

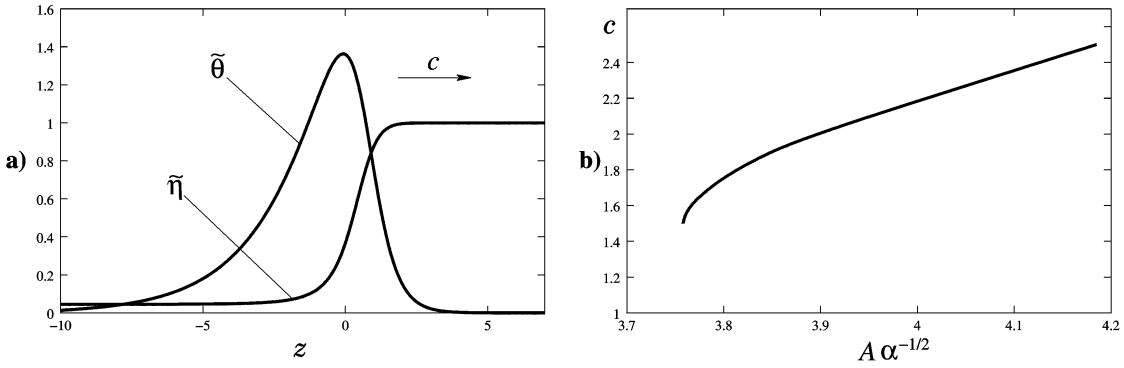

Fig. 4. (a) Solution of Eqs. (35) and (36) for $\tilde{A} = 3.76$. (b) Dependence $c(\tilde{A})$ obtained from Eqs. (35) and (36).

obtained from the numerical solution of Eqs. (35) and (36). Observe that already for $\tilde{A} \gtrsim 1.4\tilde{A}_{bT}$ the velocity of the AS agrees with Eq. (28) with accuracy better than 15%. Behind the spike region (in the region of the smooth distributions) we will have $\theta = 0$ and $\eta = 1 - (1 - \eta_{\min})e^{\alpha z/c}$. If one assumes that $\eta_{\min} = 0$, one would arrive once again at Eq. (33).

We would like to emphasize that even for $A \sim \alpha^{1/2} \ll 1$, that is, for such a small deviation of the system from thermal equilibrium, the amplitude of the AS is $\theta_{\max} \sim \alpha^{-1/2} \gg 1$ and the velocity $c \sim 1$. In other words, the AS remains a highly nonequilibrium object in the system only slightly away from thermal equilibrium.

3.1.3. Case $A \sim \alpha^{-1/2}$: oscillatory tail

In the other limiting case $A \gg 1$ the behavior of the secondary sharp distributions in the back of the AS acquires special features. This is due to the fact that for $A \gg 1$ the phase trajectory $\theta(\eta)$ in the phase plain of θ and η may pass close to the unstable fixed point (see Eq. (16)) $\theta_{h3} \simeq A$, $\eta_{h2} \simeq A^{-2}$, so the behavior of the distributions of θ and η behind the spike becomes oscillatory. In other words, θ and η will not be able to get back to the homogeneous state $\theta = \theta_h$ and $\eta = \eta_h$ at $z = -\infty$. To see that, let us introduce

$$\tilde{\theta} = \alpha^{1/2}\theta, \qquad \tilde{\eta} = \alpha^{-1}\eta,$$
$$\tilde{A} = \alpha^{1/2}A, \qquad \xi = \frac{z}{c}. \tag{37}$$

Then, we can rewrite Eqs. (22) and (23) behind the spike as follows:

$$\tilde{\theta}_\xi + \tilde{A}\tilde{\theta}^2\tilde{\eta} - \tilde{\theta} = 0, \tag{38}$$

$$\tilde{\eta}_\xi - \tilde{\theta}^2\tilde{\eta} + 1 = 0, \tag{39}$$

where we kept only the leading terms. In order for the solutions of these equations to properly match with the primary sharp distributions, we must have $\tilde{\theta} \sim e^{\xi}$ and $\tilde{\eta} \sim e^{-2\xi}$ as $\xi \to +\infty$ (see Eqs. (30) and (31)). The numerical solution of Eqs. (38) and (39) with these boundary conditions shows that at $\tilde{A} > \tilde{A}_{dT} = 0.90$ the distributions of $\tilde{\theta}$ and $\tilde{\eta}$ become oscillatory behind the spike. Thus, we conclude that the ultrafast traveling spike AS exists in a wide range $A_{bT} < A < A_{dT}$, where $A_{bT} = 3.76\alpha^{1/2}$ and $A_{dT} = 0.90\alpha^{-1/2}$. Notice that the oscillatory behavior of the distributions of θ and η behind the spike of the AS is essentially related to the Hopf bifurcation of the homogeneous state $\theta = \theta_{h3}$, $\eta = \eta_{h3}$ for $0.41\alpha^{-1/2} < A < \alpha^{-1/2}$ (see Section 2). On the other hand, for $A > \alpha^{-1/2}$ this homogeneous state becomes stable, so in that case the traveling spike AS transforms to a wave of switching from one stable homogeneous state to the other.

3.1.4. Justification of the condition $\epsilon \gg \alpha^{1/2}$ and case $\alpha = \epsilon^2$

Above we considered the case, in which the inhibitor does not diffuse. Let us see how the diffusion of the inhibitor affects the properties of the ultrafast traveling spike AS. Since the main parameters of the AS are determined by the primary supersharp

distributions, the diffusion of the inhibitor should not significantly affect these distributions. According to Eq. (23), the term $\epsilon^{-2}\,\mathrm{d}^2\eta/\mathrm{d}z^2 \sim \epsilon^{-2}\alpha^{-1}A^2$ is small compared to the leading terms which are of order $\alpha^{-2}A^2$ (see Eq. (25)) if $\epsilon^2 \gg \alpha$ regardless of A. Note that these estimates remain valid even at $A \sim A_{bT}$. In terms of the physical parameters of the problem this means that the ultrafast traveling AS will be described by the solution obtained above as long as $D_X \gg D_Y$. It is also clear that when $\alpha \sim \epsilon^2$, the properties of the AS will not change qualitatively. An interesting special case $\alpha = \epsilon^2$ which corresponds to the activator and the inhibitor with equal diffusion coefficients can be treated in an analogous way (see also [44]). The resulting equation for the supersharp distributions will have the form of Eq. (27), but without the nonlinear friction term. This equation can be solved exactly, giving in this case the velocity $\tilde{c} = 1/\sqrt{2}$ [44,45], which is in fact close to the one obtained in the case of the nondiffusing inhibitor. The explicit expression for the supersharp distributions in this case are $\tilde{\theta}_{\mathrm{ssh}} = \frac{1}{2}(1 - \tanh(\xi/2\sqrt{2}))$, $\eta_{\mathrm{ssh1}} = \frac{1}{2}(1 + \tanh(\xi/2\sqrt{2}))$, and $\eta_{\mathrm{ssh2}} = \alpha^2 A^{-2} + \mathrm{e}^{\xi/\sqrt{2}}$. The rest of the solution will be the same as in the case $\epsilon = \infty$. All this allows us to conclude that the ultrafast traveling spike AS in the Gray–Scott model exists when $\epsilon \gtrsim \alpha^{1/2}$.

3.2. *Diffusive inhibitor:* $\epsilon \ll \alpha^{1/2}$

Now let us analyze the second type of the traveling spike AS which is realized when both $\alpha \ll 1$ and $\epsilon \ll 1$, more precisely, when $\epsilon \ll \alpha^{1/2} \ll 1$.

3.2.1. *Special case* $c = 0$*: static spike autosoliton*

Observe that according to the general qualitative theory of ASs, at $\epsilon \ll 1$ static spike ASs should be realized in the Gray–Scott model [9–11]. This result is supported by the analytical and the numerical studies of the model [40,46–48,73]. For $\epsilon \ll 1$ there is a strong separation of length scales in the AS [9–11,16,57,58]. One can separate the spike region where the distribution of θ varies on the length scale of order ϵ and the periphery of the AS where η decays into the homogeneous state $\eta_{\mathrm{h}} = 1$ on the length scale of order 1. Here we will consider only the case $\epsilon^{1/2} \lesssim A \ll 1$, for more general results see [40,47,73].

Let us assume that the value of η inside the spike (on the length scale of ϵ) is close to a constant. This is a reasonable assumption as long as $\eta \gg \epsilon$ in the spike since the characteristic length scale of the variation of η is 1. Let us denote this constant value of η as η_{s}. Then, Eq. (22) with $c = 0$ and $\eta = \eta_{\mathrm{s}}$ can be solved exactly. Its solution has the form,

$$\theta(x) = \theta_{\mathrm{m}} \cosh^{-2}\left(\frac{x}{2\epsilon}\right) \quad \text{with } \theta_{\mathrm{m}} = \frac{3}{2A\eta_{\mathrm{s}}}. \tag{40}$$

On the other hand, the distribution of θ given by Eq. (40) acts in Eq. (23) as a δ-function, so away from the spike the distribution of η is given by

$$\eta(x) = 1 - \frac{3\epsilon}{\eta_{\mathrm{s}} A^2}\mathrm{e}^{-|x|}. \tag{41}$$

Now, matching this solution for $\eta(x)$ with the condition that $\eta(0) = \eta_{\mathrm{s}}$, we obtain the following expressions:

$$\theta_{\mathrm{m}} = \frac{3A}{A_b^2}\left[1 \pm \sqrt{1 - \frac{A_b^2}{A^2}}\right],$$
$$\eta_{\mathrm{s}} = \frac{A_b^2}{2A^2}\left[1 \pm \sqrt{1 - \frac{A_b^2}{A^2}}\right]^{-1}, \tag{42}$$

where

$$A_b = \sqrt{12\epsilon}. \tag{43}$$

Note that these results were also obtained in [46] by applying Melnikov analysis to Eqs (22) and (23). Similar results for a simplified version of the Gray–Scott model were obtained in [51].

From Eq. (43) one can see that at $A < A_b$ the solution in the form of the spike AS does not exist. When $A > A_b$ there are two solutions: the one corresponding to the plus sign has larger amplitude and the one corresponding to the minus sign has smaller amplitude. As was shown by Kerner and Osipov [9–11], the solutions that have smaller amplitude are always unstable, so the only interesting solution corresponds to the plus sign in Eq. (42). This solution is precisely the static spike AS. As can be seen from Eqs. (40) and

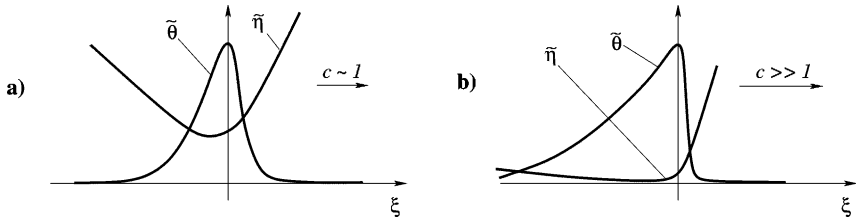

Fig. 5. Qualitative form of the traveling spike AS at $\epsilon^2 \ll \alpha \lesssim \epsilon$ for $c \sim 1$ (a) and $c \gg 1$ (b).

(41), the distribution of the activator in the AS indeed has a form of the spike whose characteristic width is of order ϵ, and the distribution of the inhibitor varies on the much larger length scale of order 1. Also, according to Eq. (42), the amplitude of the spike at A close to A_b is of order $\epsilon^{-1/2} \gg 1$ (and can in fact have huge values as ϵ gets smaller) and grows as the value of A increases. These features fundamentally differ the AS forming in Λ-systems from the AS in N-systems.

Recall that in the derivation we neglected the variation of the inhibitor inside the spike. Since the characteristic length of the variation of η is of order 1, this means that the value of $\eta = \eta_s$ in the center of the AS must be much greater than ϵ. According to Eq. (42), this is indeed the case as long as $A \ll 1$, so the solution obtained above is a good approximation to the actual solution in this case. Note that in the case $A \sim 1$ a modified asymptotic procedure may be used to obtain the solution in the form of the static spike AS for $\epsilon \ll 1$ [40,47,48,73]. This asymptotic procedure shows that the AS exists only for $A < A_d = 1.35$ in this limit. For $A > A_d$ the static spike AS starts to split in the Gray–Scott model [40,47,48,73].

3.2.2. Case $c \neq 0$

Now we will show that when $\epsilon \ll 1$ and α small enough, in addition to the static spike AS there are solutions in the form of the traveling spike AS which propagates with constant velocity whose magnitude is $c \gtrsim l/\tau_\theta$.

Since $\epsilon \ll 1$, it is natural to separate the distributions of θ and η into sharp and smooth distributions. In the spike region we introduce the scaled variables which will describe the sharp distribution (inner solution),

$$\tilde{\theta} = \epsilon\theta, \qquad \tilde{\eta} = \epsilon^{-1}\eta. \tag{44}$$

In terms of these variables, Eqs. (22) and (23) become

$$\tilde{\theta}_{zz} + c\tilde{\theta}_z + A\tilde{\theta}^2\tilde{\eta} - \tilde{\theta} = 0, \tag{45}$$

$$\tilde{\eta}_{zz} - \tilde{\theta}^2\tilde{\eta} = 0, \tag{46}$$

where we assumed that $\epsilon \ll \alpha^{1/2}$ and $\theta^2\eta \gg 1$ in the spike and kept only the leading terms. According to Eq. (46), the asymptotic behavior of $\tilde{\eta}$ at large $|z|$ is

$$\tilde{\eta} \simeq \kappa_\pm z, \quad z \to \pm\infty, \tag{47}$$

where $\kappa_\pm$ are some constants. Therefore, the distributions of $\tilde{\theta}$ and $\tilde{\eta}$ in the spike will qualitatively have the form as shown in Fig. 5.

It is convenient to introduce the following variables:

$$\bar{\theta} = \frac{\tilde{\theta}}{A}, \qquad \bar{\eta} = \tilde{\eta} + \frac{\tilde{\theta}}{A}. \tag{48}$$

Then, Eq. (46) can be written as

$$\bar{\eta}_{zz} = \bar{\theta} - c\bar{\theta}_z. \tag{49}$$

Because of the translational invariance, we have the freedom to choose the position of the spike. We will do it in such a way that the maximum of $\bar{\theta}$ is located at $z = 0$, that is, we have $\bar{\theta}_z(0) = 0$. Also, according to Eq. (49), we can add an arbitrary function $a + bz$ to its solution, so we may replace $\bar{\eta} \to \bar{\eta} + \bar{\eta}_s + \kappa z$, where $\bar{\eta}_s$ and κ are arbitrary constants, and require that $\bar{\eta}(0) = \bar{\eta}_z(0) = 0$, so the function $\bar{\eta}(z)$ is completely determined by $\bar{\theta}(z)$. In view of all this, Eq. (45) becomes

$$\bar{\theta}_{zz} + c\bar{\theta}_z + A^2\bar{\theta}^2(\bar{\eta}_s + \kappa z + \bar{\eta} - \bar{\theta}) - \bar{\theta} = 0. \tag{50}$$

According to Eq. (47), we have $\bar{\eta}_z(\pm\infty) = \kappa_\pm - \kappa$. This implies that $\bar{\eta}_z(+\infty) - \bar{\eta}_z(-\infty) = \kappa_+ - \kappa_-$. Integrating Eq. (49) over z, we obtain an integral representation of this condition,

$$\int_{-\infty}^{+\infty} \bar{\theta}\,\mathrm{d}z = \kappa_+ - \kappa_-. \tag{51}$$

By a similar integration, the value of κ is determined as

$$\kappa = \kappa_- + \int_{-\infty}^{0} \bar{\theta}\,\mathrm{d}z. \tag{52}$$

To study the solutions of Eqs. (49) and (50), we use the mechanical analogy. Eq. (50) can be considered as an equation of motion for a particle of unit mass with the coordinate $\bar{\theta}$ and time z in the potential $U = -\frac{1}{2}\bar{\theta}^2 + \frac{1}{3}A^2\bar{\eta}_\mathrm{s}\bar{\theta}^3 - \frac{1}{4}A^2\bar{\theta}^4$ in the presence of friction, with the friction coefficient c, and an external time-dependent force $-A^2\bar{\theta}^2[\kappa z + \bar{\eta}(z)]$. For $\bar{\eta}_\mathrm{s} > 2A^{-1}$ the potential has two maxima at $\bar{\theta} = 0$ and $\bar{\theta} = \bar{\theta}_\mathrm{m}$, and a minimum in between. The particle slides down from the maximum of the potential at $\bar{\theta} = 0$ and after an excursion toward $\bar{\theta} = \bar{\theta}_\mathrm{max} < \bar{\theta}_\mathrm{m}$ at $z = 0$ returns to $\bar{\theta} = 0$. Notice that since by definition $\bar{\eta}(0) = \bar{\eta}_z(0) = 0$, the value of $\bar{\eta}$ should be rather small in the spike region, so one could think of the second term in $-A^2\bar{\theta}^2[\kappa z + \bar{\eta}(z)]$ as a small perturbation.

In the presence of friction the external time-dependent force acting in Eq. (50) must be such that it accelerates the particle at some portion of the trajectory. According to Eq. (49) and the fact that $\bar{\theta}_z < 0$ for $z > 0$, we have $\bar{\eta} > 0$ for those values of z. Since the values of κ relevant to our analysis are positive (see below), in the portion of the trajectory where $z > 0$ the external force does accelerate the particle. All the kinetic energy that is gained by the particle during this part of the motion must be dissipated by the friction force, so that the particle arrives at $\bar{\theta} = 0$ with zero velocity. This defines the precise value of the friction coefficient c as a function of $\bar{\eta}_\mathrm{s}$ and κ. Recall that in addition the distribution $\bar{\theta}(z)$ must satisfy the integral condition in Eq. (51), so in fact we are not free to choose the value of $\bar{\eta}_\mathrm{s}$. Thus, for given values of $\kappa_\pm$ there may exist only a discrete set of the velocities c.

Away from the spike θ is zero, and η is described by the smooth distributions (outer solutions). If we introduce the variable $\zeta = \epsilon z$, we can write Eq. (23) in the form,

$$\eta_{\zeta\zeta} + \beta^{-1}c\eta_\zeta + 1 - \eta = 0, \tag{53}$$

where $\beta = \alpha/\epsilon$. We should choose such a solution of this equation that correctly matches with the sharp distribution in the spike. To do that, we use the fact that to order ϵ the value of $\eta(0) = 0$, so the smooth distribution of η is

$$\eta(\zeta) = 1 - \exp(-\kappa_\pm\zeta), \tag{54}$$

where

$$\kappa_\pm = \frac{c \pm \sqrt{c^2 + 4\beta^2}}{2\beta}, \tag{55}$$

and one should take κ_+ if $\zeta > 0$, or κ_- otherwise. Note that for $\beta \sim 1$ and $c \sim 1$ we have $\kappa_\pm \sim 1$. From Eq. (54) one can see that when ζ approaches the spike region, we have $\eta \simeq \kappa_\pm\zeta = \epsilon\kappa_\pm z$. This means that we should use the values of $\kappa_\pm$ given by Eq. (55) in solving the inner problem given by Eqs. (49)–(52).

3.2.3. Case $\epsilon A^2 \lesssim \alpha \ll \epsilon A$: bifurcation of the static and traveling autosolitons

Eqs. (50)–(52) are difficult to deal with and in general can only be treated numerically. Such a treatment was performed by Reynolds et al. [40,73], who also derived these equations in a different context. The problem can be significantly simplified in the case $A \ll 1$. In this case there is a small factor of A^2 multiplying a number of terms in Eq. (50). It can be partially compensated by choosing $\bar{\eta}_\mathrm{s} \sim A^{-2} \gg 1$. If we neglect the other terms containing A^2 and put $c = 0$ in Eq. (50), we can solve this equation (together with Eq. (51)) exactly. The result is

$$\bar{\theta}_0(z) = \frac{\kappa_+ - \kappa_-}{4}\cosh^{-2}\left(\frac{z}{2}\right),$$
$$\bar{\eta}_\mathrm{s} = \frac{6}{A^2(\kappa_+ - \kappa_-)}. \tag{56}$$

Note that according to Eqs. (52) and (56), we may put $\kappa = (\kappa_+ + \kappa_-)/2 = c/2\beta$.

The equation describing the small deviations $\delta\bar{\theta} = \bar{\theta} - \bar{\theta}_0$ due to the order A^2 terms that were dropped in the derivation of Eq. (56) can be obtained by the linearization of Eq. (50) around $\bar{\theta}_0$. Assuming that $c \ll 1$ and retaining only the term that gives the nontrivial contribution to c, we get

$$\left[-\frac{\mathrm{d}^2}{\mathrm{d}z^2} - 2A^2\bar{\eta}_\mathrm{s}\bar{\theta}_0 + 1\right]\delta\bar{\theta} = A^2\bar{\theta}_0^2\kappa z + c\frac{\mathrm{d}\bar{\theta}_0}{\mathrm{d}z}. \quad (57)$$

The operator in the left-hand side of this equation has an eigenvalue zero, corresponding to the translational mode $\delta\bar{\theta} = \mathrm{d}\bar{\theta}_0/\mathrm{d}z$. Therefore, in order for Eq. (57) to have a solution, its right-hand side must be orthogonal to this translational mode. The operator in Eq. (57) is self-adjoint, so in order to get the solvability condition for this equation, we should require that the integral of its right-hand side multiplied by $\mathrm{d}\bar{\theta}_0/\mathrm{d}z$ be equal to zero. With the use of Eq. (56), this gives us the velocity c as a function of $\kappa_\pm$

$$c = \tfrac{1}{6}A^2(\kappa_+^2 - \kappa_-^2). \quad (58)$$

To determine the velocities that are actually realized in the traveling spike AS, we need to take into account the matching conditions that are given by Eqs. (55). With the use of these equations, Eq. (58) becomes

$$c = 2\beta\sqrt{\frac{\beta^2}{\beta_T^2} - 1}, \quad \beta_T = \frac{A^2}{3}. \quad (59)$$

Since in the derivation of this equation we assumed that $c \ll 1$, it will be valid only for $\beta \ll A$. Note that similar results were recently obtained in the geometric analysis of pairs of interacting pulses [49,50].

Two observations can be made from Eq. (59). First, at some $\beta = \beta_T(A)$ (or at some $A = A_T(\beta)$) the velocity of the AS becomes zero. Since this happens for $\beta \sim A^2$ and $\alpha \gg \epsilon^2$, we have $\epsilon^{1/2} \ll A \ll 1$, so there is also a solution with $c = 0$ (see Section 3.2.1). The presence of a point where the velocity of the *traveling* solution goes to zero therefore signifies a bifurcation of the static AS. Second, according to Eq. (59) the velocity of the obtained solution is a *decreasing* function of A (or an increasing function of β). In contrast, we would expect the velocity of the traveling spike AS to be an *increasing* function of the excitation level A.

Let us consider an iterative map that takes c, substitutes it to Eq. (55) with the fixed $\kappa_+ + \kappa_-$, calculates κ and uses Eq. (58) to give the new value of c. This map should mimic the stability of the AS. Indeed, since the distribution of the inhibitor is controlled by the activator, a distribution of θ that is close to a solution of Eq. (50) with a given c should produce a distribution of η which is close to that in Eq. (54) with Eq. (55), which will in turn affect θ. Clearly, those c given by Eq. (59) (or $c = 0$) are fixed points of this map. However, an analysis of this map shows that an arbitrarily small deviation of c from that given by Eq. (59) will lead to the unlimited growth of c if the deviation is positive, or to zero if the deviation is negative. In other words, the fixed point given by Eq. (59) is unstable. Also, one can easily see that for $A < A_T$ the fixed point at $c = 0$ is stable for $A < A_T$ (or $\beta > \beta_T$) and unstable otherwise. This means that the solution with nonzero velocity we found above and the static solution at $A > A_T$ or $\beta < \beta_T$ should be unstable. Therefore, the stable traveling solutions should have the velocity $c \gtrsim 1$ and may exist both when $A < A_T$ and $A > A_T$. Also, when $A > A_T$, the solutions with $c = 0$ should be unstable, so the static spike AS spontaneously transforms into the traveling spike AS, whose speed $c \gtrsim 1$. These conclusions are also supported by the numerical simulations of Eqs. (19) and (20).

3.2.4. Case $\alpha \ll \epsilon A$: ultrafast traveling autosoliton

Above we considered the situation in which $c \ll 1$. Let us now study another possibility: $c \gg 1$. In this case the distribution of $\bar{\theta}$ will become strongly asymmetric (see Fig. 5(b)). Indeed, according to Eq. (50), we will have $\bar{\theta} \sim \mathrm{e}^{-cz}$ at $z \to +\infty$ and $\bar{\theta} \sim \mathrm{e}^{z/c}$ at $z \to -\infty$. In other words, we can once again separate the distributions of $\bar{\theta}$ and $\bar{\eta}$ into the regions of the supersharp distributions (in the front of the spike) and the sharp distributions (in the back of the spike). In the region of the supersharp distributions the supersharp front will have the width of order $c^{-1} \ll 1$. Let us introduce $\xi = cz$. Then, we can write Eq. (49) integrated over ξ and Eq. (50) as

$$\bar{\theta}_{\xi\xi} + \bar{\theta}_\xi + c^{-2}A^2\bar{\theta}^2(\bar{\eta}_\mathrm{s} + \bar{\eta} - \bar{\theta}) = 0, \quad (60)$$

$$\bar{\eta}_\xi = -\bar{\theta} + \bar{\theta}_\mathrm{max}, \quad (61)$$

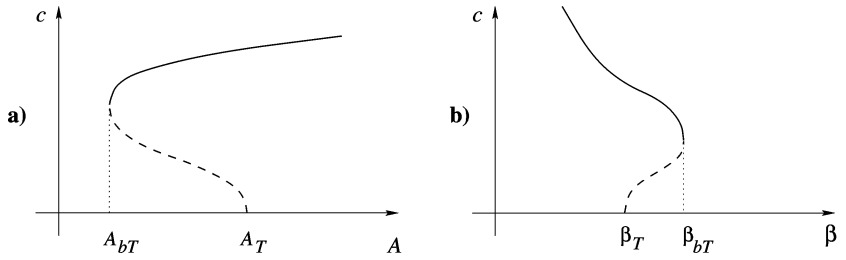

Fig. 6. Qualitative form of the dependence $c(A)$ (a) and the dependence $c(\beta)$ (b) for the traveling spike AS.

where we retained only the leading terms and moved the point where $\bar{\theta}$ attains its maximum value to minus infinity (this amounts to putting $\kappa = 0$ in Eq. (60) and redefining the boundary condition for $\bar{\eta}$ to be $\bar{\eta}(-\infty) = \bar{\eta}_\xi(-\infty) = 0$). One can see that by rescaling $\bar{\theta}$ and $\bar{\eta}$ with $\bar{\theta}_{\max}$ all the A- and $\bar{\theta}_{\max}$-dependence from Eqs. (60) and (61) can be absorbed into c. These equations have a solution in the form of a supersharp front connecting $\bar{\theta} = 0$ ahead of the front with $\bar{\theta} = \bar{\theta}_{\max}$ behind the front only when $\bar{\eta}_s = \bar{\theta}_{\max}$. In this case we have $\bar{\eta}_\xi(+\infty) = \bar{\theta}_{\max}$ (see Eq. (61)), what corresponds to $\kappa_- = 0$ and $\kappa_+ = c\beta^{-1}$. According to Eq. (55), these values of $\kappa_\pm$ can only be realized when $c \gg \beta$, with $\bar{\theta}_{\max} = \beta^{-1}$. Note that the fact that $\bar{\eta}_s = \bar{\theta}_{\max}$ behind the supersharp front means that $\tilde{\eta}$ exponentially decays to zero at $\xi \to -\infty$.

The numerical solution of Eqs. (60) and (61) shows that the velocity of the supersharp front is

$$c = 1.22A\beta^{-1}. \tag{62}$$

Since by assumption $c \gg 1$, we must have $\beta \ll A$. Recall that in the derivation we also assumed that $c \gg \beta$. According to Eq. (62), this leads to $\beta^2 \ll A$. Since, as we will show in Section 3.2.5, the solution in the form of the traveling AS exists only when $\beta \lesssim 1$, this condition is always satisfied when $\beta \ll A$. Note that the numerical solution of Eqs. (60) and (61) in the form of the supersharp front differs from $\bar{\theta}_{ssh} = \frac{1}{2}[1 - \tanh(0.44\xi)]$ by less than 0.5%.

In the region of the sharp distributions the characteristic length scale of the variation of $\bar{\theta}$ is c, so we can neglect the term $\bar{\theta}_{zz}$ in Eq. (50). Recalling that $\tilde{\eta} = 0$ in this region, we can write the solution of this equation that represents the sharp distribution of θ behind the supersharp front as $\bar{\theta}_{sh} = \bar{\theta}_{\max} e^{z/c}$, where we assumed that the supersharp front is located at $z = 0$.

When the value of A is decreased, the velocity of the unstable traveling solution grows and the velocity of the stable traveling solution decreases until they reach the value of order 1 when the approximations used in deriving the above equations become invalid. According to Eq. (62), this will happen at $A \sim \beta$, so at some $A = A_{bT} \sim \beta$ the solution in the form of the traveling spike AS will disappear. Therefore, the velocity of the traveling spike AS as a function of A or β should have the form as shown in Fig. 6.

For $\beta \lesssim 1$ the traveling AS exists at $A \gtrsim \beta$. On the other hand, for these values of β the static spike AS remains stable up to the values of $A \sim \beta^{1/2}$ (see Eq. (59) and the discussion below). Therefore, for $\beta \lesssim A \lesssim \beta^{1/2}$ the static spike AS will coexist with traveling.

3.2.5. Case $A \sim \epsilon^{-1}$, $\alpha \lesssim \epsilon$: oscillatory tail

When the speed of the traveling spike AS increases, the behavior of the distributions of θ and η in the back of the AS changes in the way similar to the case of the ultrafast traveling spike AS (Section 3.1.3). For large enough values of A the sharp distributions in the back of the spike become oscillatory. To see that let us introduce the variables,

$$\tilde{\theta} = \epsilon^{1/2}\theta, \qquad \tilde{\eta} = \epsilon^{-1}\eta,$$
$$\tilde{A} = \epsilon^{1/2}A, \qquad \tilde{c} = \epsilon^{1/2}c, \qquad \xi = \frac{z}{c}, \tag{63}$$

where c is given by Eq. (62). Then, keeping only the leading terms, we can write Eqs. (22) and (23) in the region of the sharp distributions as follows:

$$\tilde{\theta}_\xi + \tilde{A}\tilde{\theta}^2\tilde{\eta} - \tilde{\theta} = 0, \tag{64}$$

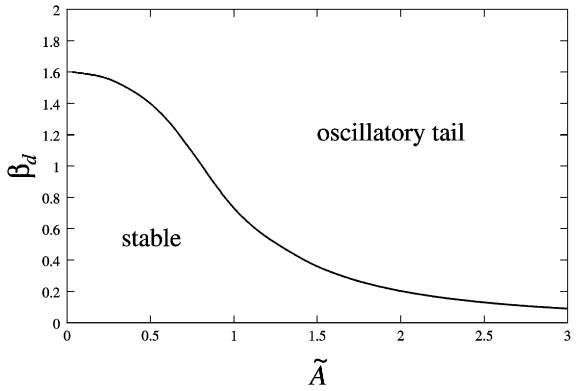

Fig. 7. Dependence $\beta_d(\tilde{A})$ for the traveling spike AS.

$$\frac{1}{\tilde{c}^2}\tilde{\eta}_{\xi\xi} + \frac{1}{\beta}\tilde{\eta}_{\xi} - \tilde{\theta}^2\tilde{\eta} - 1 = 0. \tag{65}$$

To match the solutions of these equations with the supersharp distributions we must have $\eta \to 0$ for $\xi \to +\infty$, so $\tilde{\theta} \sim \mathrm{e}^{\xi}$ and $\tilde{\eta} \sim \mathrm{e}^{-2\xi}$ for large ξ. Similarly, in order for the distributions of $\tilde{\theta}$ and $\tilde{\eta}$ to properly match with the smooth distributions, for $\xi \to -\infty$ we must have $\tilde{\theta}(-\infty) = 0$ and $\tilde{\eta}_{\xi} = -\beta$ (see Eq. (55) with $c \gg 1$). With these boundary conditions Eqs. (64) can then be solved numerically. As a result, we find the values of $\beta = \beta_d$ as a function of $\tilde{A}$ at which the behavior of the distributions of $\tilde{\theta}$ and $\tilde{\eta}$ in the back of the spike changes to oscillatory. The dependence $\beta_d(\tilde{A})$ is plotted in Fig. 7. From this figure one can also see that the solution in the form of the traveling spike AS exists only at $\beta < \beta_c \simeq 1.6$. The analysis of Eqs. (64) and (65) also shows that for $\tilde{A} \gg \beta^{3/2}$ the second derivative of $\tilde{\eta}$ in Eq. (65) can be dropped, so the problem reduces to that given by Eqs. (38) and (39) with $\tilde{A}$ replaced by $\tilde{A}\beta^{1/2}$. Therefore, for large enough values of $\tilde{A}$ we should have $\beta_d \simeq 0.81\tilde{A}^{-2}$. The numerical simulations of Eqs. (19) and (20) show that the onset of the oscillatory behavior in the back of the spike in the traveling spike AS results in the splitting of the AS as it moves [47].

3.2.6. Case $\alpha \sim \epsilon$, $A \sim 1$: qualitative considerations

So far, we concentrated on the situations in which either $c \ll 1$ or $c \gg 1$. We gave an argument that only the solutions with $c \gg 1$ should be stable and can be realized only if $\beta \lesssim 1$ and $\beta \ll A$ (Section 3.2.4). As was shown in Section 3.2.5, in the case $A \gg 1$ the solution in the form of the traveling spike AS will exist only if $\beta < \beta_c \sim 1$. It is clear that qualitatively these conclusions can also be made when both $A \sim 1$ and $\beta \sim 1$, what corresponds to $c \sim 1$. In this case the AS will not be able to propagate at $A < A_{bT} \sim 1$ and will transform into the static AS. On the other hand, for $A > A_{dT} \sim 1$ the traveling spike AS will start splitting. When the value of β is increased, the value of A_{bT} will grow and the value of A_{dT} will decrease, so at some $\beta = \beta_c$ the solution in the form of the traveling spike AS will disappear. This conclusion is supported by the numerical simulations of Eqs. (19) and (20), with the value of β_c found to be very close to the one obtained in the preceding paragraph.

Let us give some heuristic arguments for explaining the reasons for stopping the traveling spike AS at $A < A_{bT}$ or splitting at $A > A_{dT}$. Consider Eqs. (49) and (50), using the mechanical analogy. Let us see what happens as the value of A decreases when $c \sim 1$. In this case the external force $-A^2\bar{\theta}(\kappa z + \bar{\eta})$ accelerating the particle on the way from $\bar{\theta}_{\max}$ to 0 becomes smaller (see Eq. (50)), while the friction force remains the same. When the value of A becomes small enough, the dissipation will exceed the acceleration, so the particle will not be able to reach $\bar{\theta} = 0$ and the solution traveling with constant velocity will disappear. On the other hand, as long as $A_b < A < A_d$, where A_b is the point where the solution in the form of the static spike AS disappears and A_d the point where the static spike AS starts splitting [47,48], the static solution will exist, so the traveling AS will be able to stop and transform into static when the value of A is decreased.

According to the definition of $\bar{\theta}$, when z is close to zero, the time-dependent external force is dominated by $-A^2\bar{\theta}^2\kappa z$, which is positive in some interval $z_0 < z < 0$. This means that the particle is accelerated by this force before it stops at $\bar{\theta} = \bar{\theta}_{\max}$. If the value of A is big enough and the friction coefficient $c \sim 1$, the forces from the potential U and the friction may not be enough to stop the particle before it reaches the maximum of the potential at $\bar{\theta} = \bar{\theta}_{\mathrm{m}}$. Then, if the particle moves past $\bar{\theta}_{\mathrm{m}}$, it will keep on moving toward plus infinity and will never be able to return to

$\bar{\theta} = 0$. This means that the solution in the form of the traveling spike AS must disappear at some $A = A_{dT} \sim 1$. Notice that the same argument can be applied to the static AS at $A = A_d$, so this bifurcation point should indeed correspond to the onset of splitting. For further discussion of splitting of the traveling pulses see also [49,50,52].

4. Numerical simulations

The numerical simulations of Eqs. (19) and (20) confirm the conclusions of Section 3 about the existence of the traveling spike ASs. A sufficiently strong localized stimulus applied to one boundary of the system of large but finite size in the homogeneous state results in the formation of a traveling spike AS. The properties as well as the behavior of this AS mainly depend on the relationship between α and ϵ.

Fig. 8(a) shows the distributions of θ and η in the form of an ultrafast traveling spike AS for $\epsilon = \infty$, $\alpha = 0.05$, and $A = 2$. The speed of this AS was found to be $c = 7.3$, which agrees within 5% with that of Eq. (28). Also, the shape of the traveling spike AS is in agreement with the predictions of Section 3.1.

Fig. 8(b) shows the distributions of θ and η in the form of the traveling spike AS with the diffusion precursor. It shows the result of the numerical solution of Eqs. (19) and (20) for $\epsilon = 0.05$, $\alpha = 0.05$ and $A = 2$. The speed of this AS was found to be $c = 1.26$, much smaller than the speed of the ultrafast traveling AS discussed in the preceding paragraph. The shape of the slower traveling spike AS agrees with that found in the asymptotic theory (see Section 3.2). Fig. 9 shows the dependence of the AS speed c on A at different values of α obtained from the numerical solution of Eqs. (19) and (20) with $\epsilon = 0.05$. Note that the curves $c(A)$ in Fig. 9 terminate at sufficiently large values of A. This is due to the fact that when the value of A exceeds a certain critical value which depends on α, the traveling AS starts splitting as it moves. This is in agreement with the predictions of Section 3.2.5 about the disappearance of the solution in the form of the traveling AS due to the onset of the oscillations in the back of the spike for sufficiently large values of A.

Two ultrafast traveling ASs without the diffusion precursors moving towards each other annihilate. A much more diverse situation is realized in the case $\epsilon^2 \lesssim \alpha \lesssim \epsilon$ when the traveling spike AS with the diffusion precursor exist. Here the ASs moving towards each other can annihilate before colliding or bounce off each other and start traveling in the opposite direction as a result of the interaction via the diffusion of the inhibitor (a diffusion precursor). Also, as was shown in Section 3.2.3, the static spike AS may spontaneously transform into traveling when the value of α is decreased. This phenomenon was studied by Osipov and Severtsev in [51] in a simplified version of the Gray–Scott model and is observed in our simulations of Eqs. (19) and (20) as well. Since for $\epsilon = 0.05$ the value of A_d at which the static spike AS starts splitting is $A_d = 1.49$ [47], there exists a parameter

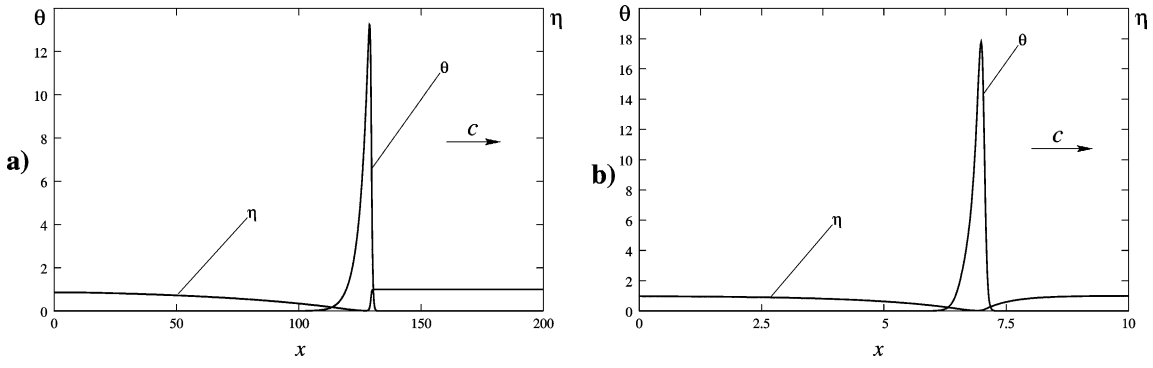

Fig. 8. Two types of traveling spike AS: case $\epsilon \gg \alpha^{1/2}$ (a) and $\epsilon \sim \alpha$ (b). Results of the numerical solution of Eqs. (12) and (13). In (a) $L = 0$, $\alpha = 0.05$, $A = 2$, length is measured in the units of l. In (b) $\epsilon = 0.05$, $\alpha = 0.05$, $A = 2$, length is measured in the units of L.

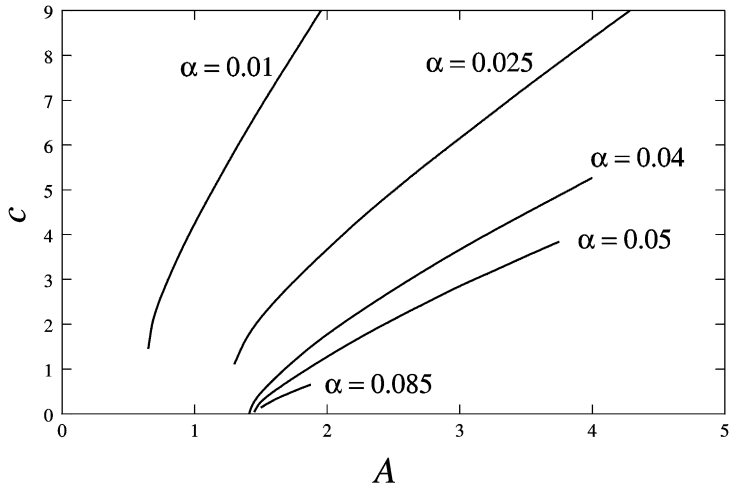

Fig. 9. Dependences $c(A)$ for the traveling spike AS at different values of α obtained from the numerical solution of Eqs. (19) and (20) with $\epsilon = 0.05$.

region where it is possible to excite both the static and the traveling ASs simultaneously. According to Fig. 9, when the value of A becomes sufficiently close to A_d, the speed of the traveling spike AS may go to zero for a range of α. When $\epsilon = 0.05$, this happens when $0.03 < \alpha < 0.06$. According to the simulations, at $\epsilon = 0.05$ and $A = 1.34$ the bifurcation of the static and the traveling ASs changes from subcritical to supercritical, so at higher values of A their coexistence is no longer possible.

5. Conclusion

In conclusion, we have asymptotically constructed solutions in the form of the traveling spike ASs in the Gray–Scott reaction–diffusion model of an autocatalytic chemical reaction. We found that the traveling spike ASs exist in the Gray–Scott model in a wide range of the system's parameters and can be excited even in the system only weakly away from thermal equilibrium.

The properties of the traveling spike ASs in the Gray–Scott model are mainly determined by the ratio of the diffusion coefficients of the activator and the inhibitor. When the inhibitor does not diffuse (or, more precisely, when $\alpha \lesssim \epsilon^2$), the ultrafast traveling spike ASs without the diffusion precursor are realized at $\alpha^{1/2} \lesssim A \lesssim \alpha^{-1/2}$. These ASs have large amplitude $\theta_{\max} \sim A\alpha^{-1}$ and speed $c \sim A\alpha^{-1/2} \gtrsim 1$. When the inhibitor diffusion coefficient is much greater than that of the activator (or, more precisely, when $\epsilon^2 \ll \alpha \lesssim \epsilon$) the traveling spike ASs with the diffusion precursor are realized at $\alpha\epsilon^{-1} \lesssim A \lesssim \alpha^{-1/2}$. The amplitude of these ASs $\theta_{\max} \sim A\alpha^{-1}$ is also large and the speed $c \sim A\epsilon\alpha^{-1} \gtrsim 1$. Also, in this case the solutions in the form of the static spike ASs, which are a special case of the traveling wave solutions with speed $c = 0$, are realized. We found that in a wide parameter region the traveling spike ASs can coexists with static.

We would like to emphasize that the properties of the traveling spike ASs in the Gray–Scott model differ fundamentally from those of the traveling ASs in N-systems, such as the FitzHugh–Nagumo model, for example. In N-systems the traveling ASs have the form of broad pulses with sharp fronts and backs. Their amplitude is determined by the nullcline of the activator and cannot exceed the value of order 1. Similarly, their speed is bounded by a value of order 1 and is determined by the value of the inhibitor in the front of the AS. In contrast, in the Gray–Scott model the traveling ASs have the form of spikes, whose amplitude depends on the ratio of the time scales of the activator and the inhibitor and can have huge values. Also, the

speed of these ASs is typically greater than the value of order 1 and can become much greater than that of the ASs forming in N-systems.

Let us point out that the difference between the form of the traveling spike ASs in the Gray–Scott model and the FitzHugh–Nagumo-type models is the consequence of the difference in the shape of the activator nullcline in these systems. This suggests that by adding an extra term that determines the shape of the nullcline one can effectively control the type of the traveling ASs forming in the system. Specifically, in the Gray–Scott model one can introduce an extra term $-B\theta^3$ in the right-hand side of Eq. (19). Then, by changing the parameter B from 0 to a value of order 1 one can continuously go from a Λ-system to an N-system. In doing so, one can change the speed of the traveling spike ASs by several orders of magnitude! Thus, by changing the form of the activator nullcline one can exercise a sensitive control over the traveling wave solutions. This may be an important adaptive mechanism in biological systems.

Doelman et al. [46] performed an analysis of the static spike ASs in the Gray–Scott model using Melnikov analysis. In [46] Doelman et al. made a statement that the traveling spike ASs do not exist in the Gray–Scott model. While this statement is correct in the parameter region $\alpha \sim \epsilon^{2(2-\beta)/(4-\beta)}$, $A \sim \epsilon^{2(1-\beta)/(4-\beta)}$ with $\epsilon \ll 1$ and $0 \leq \beta < 1$ studied by them, it is not true in general. Indeed, in our paper we found *two different types* of the traveling spike ASs. The more so, we found *coexistence* of the traveling spike ASs with static.

References

[1] G. Nicolis, I. Prigogine, Self-organization in Nonequilibrium Systems, Wiley, New York, 1977.
[2] V.A. Vasiliev, Y.M. Romanovskii, D.S. Chernavskii, V.G. Yakhno, Autowave Processes in Kinetic Systems, VEB Deutscher Verlag der Wissenschaften, Berlin, 1987.
[3] R.J. Field, M. Burger (Eds.), Oscillations and Traveling Waves in Chemical Systems, Wiley, New York, 1985.
[4] J.D. Murray, Mathematical Biology, Springer, Berlin, 1989.
[5] M.C. Cross, P.S. Hohenberg, Rev. Mod. Phys. 65 (1993) 851.
[6] A.S. Mikhailov, Foundations of Synergetics, Springer, Berlin, 1990.
[7] R. Kapral, K. Showalter, Chemical Waves and Patterns, Kluwer Academic Publishers, Dordrecht, 1995.
[8] B.S. Kerner, V.V. Osipov, in: W. Ebeling, H. Ulbricht (Eds.), Nonlinear Irreversible Processes, Springer, Berlin, 1986.
[9] B.S. Kerner, V.V. Osipov, Sov. Phys. Usp. 32 (1989) 101.
[10] B.S. Kerner, V.V. Osipov, Sov. Phys. Usp. 33 (1990) 3.
[11] B.S. Kerner, V.V. Osipov, Autosolitons: A New Approach to Problem of Self-organization and Turbulence, Kluwer Academic Publishers, Dordrecht, 1994.
[12] F.J. Niedernostheide (Ed.), Nonlinear Dynamics and Pattern Formation, Semiconductors and Devices, Springer, Berlin, 1994.
[13] M. Bode, H.G. Purwins, Physica D 86 (1995) 53.
[14] M. Gorman, M. el Hamdi, K.A. Robbins, Combust. Sci. Technol. 98 (1994) 37.
[15] K.J. Lee, W.D. McCormick, Q. Ouyong, H.L. Swinney, Science 261 (1993) 192.
[16] B.S. Kerner, V.V. Osipov, Sov. Phys. JETP 47 (1978) 874.
[17] B.S. Kerner, V.V. Osipov, Sov. Phys. Semicond. 13 (1979) 424.
[18] B.S. Kerner, V.V. Osipov, Sov. Phys. JETP 52 (1980) 1122.
[19] S. Koga, Y. Kuramoto, Prog. Theoret. Phys. 63 (1980) 106.
[20] B.S. Kerner, V.V. Osipov, Sov. Phys. JETP 62 (1985) 337.
[21] P. Gray, S. Scott, Chem. Eng. Sci. 38 (1983) 29.
[22] A. Gierer, H. Meinhardt, Kybernetik 12 (1972) 30.
[23] P.G. FitzHugh, Biophys. J. 1 (1961) 445.
[24] J. Rinzel, J.B. Keller, Biophys. J. 13 (1973) 1313.
[25] P.J. Ortoleva, J. Ross, J. Chem. Phys. 63 (1975) 3398.
[26] B.S. Kerner, V.V. Osipov, Sov. Phys. JETP 56 (1982) 1275.
[27] B.S. Kerner, V.V. Osipov, Mikroelektronika 12 (1983) 512.
[28] E.M. Kuznetsova, V.V. Osipov, Phys. Rev. E 51 (1995) 148.
[29] K. Krischer, A. Mikhailov, Phys. Rev. Lett. 73 (1994) 3165.
[30] P. Schutz, M. Bode, V.V. Gafiichuk, Phys. Rev. E 52 (1995) 4465.
[31] V.V. Osipov, Physica D 93 (1996) 143.
[32] A.L. Dubitskii, B.S. Kerner, V.V. Osipov, Sov. Phys. Dokl. 34 (1989) 906.
[33] V.V. Osipov, Phys. Rev. E 48 (1993) 88.
[34] V.V. Osipov, C.B. Muratov, Phys. Rev. Lett. 75 (1995) 388.
[35] C.B. Muratov, V.V. Osipov, Phys. Rev. E 53 (1996) 3101.
[36] B. Katz, Nerve, Muscle, and Synapse, McGraw-Hill, New York, 1966.
[37] P.M. Wood, J. Ross, J. Chem. Phys. 82 (1985) 1924.
[38] M.N. Vinoslavskii, Sov. Phys. Solid State 31 (1989) 1461.
[39] H. Purwins, et al., Phys. Lett. A 136 (1989) 480.
[40] W.N. Reynolds, J.E. Pearson, S. Ponce-Dawson, Phys. Rev. Lett. 72 (1994) 2797.
[41] J.E. Pearson, Science 261 (1993) 189.
[42] P.C. Fife. Dynamics of Internal Layers and Diffusive Interfaces, Society for Industrial and Applied Mathematics, Philadelphia, 1988.
[43] J.K. Hale, L.A. Peletier, W.C. Troy, SIAM J. Appl. Math. 61 (2000) 102.
[44] J.H. Merkin, M.A. Sadiq, IMA J. Appl. Math. 57 (1996) 273.
[45] E. Ben-Jacob, et al., Physica D 14 (1985) 348.
[46] A. Doelman, T.J. Kaper, P. Zegeling, Nonlinearity 10 (1997) 523.
[47] C.B. Muratov, V.V. Osipov, CAMS Rep. 9900-10, NJIT, Newark, NJ. LANL archive: patt-sol/9804001.
[48] C.B. Muratov, V.V. Osipov, J. Phys. A 33 (2000) 8893.

[49] A. Doelman, W. Eckhaus, T.J. Kaper, SIAM J. Appl. Math. 61 (2000) 1080.
[50] A. Doelman, W. Eckhaus, T.J. Kaper, SIAM J. Appl. Math. 61 (2001) 2036.
[51] V.V. Osipov, A.V. Severtsev, Phys. Lett. A 227 (1997) 61.
[52] Y. Nishiura, D. Ueyama, Physica D 130 (1999) 73.
[53] M. Gorman, M. el Hamdi, K.A. Robbins, Combust. Sci. Technol. 98 (1994) 71.
[54] M. Gorman, M. el Hamdi, K.A. Robbins, Combust. Sci. Technol. 98 (1994) 79.
[55] K.J. Lee, W.D. McCormick, J.E. Pearson, H.L. Swinney, Nature 369 (1994) 215.
[56] K.J. Lee, H.L. Swinney, Phys. Rev. E 51 (1995) 1899.
[57] B.S. Kerner, V.V. Osipov, Biophysics (USSR) 27 (1982) 138.
[58] B.S. Kerner, V.V. Osipov, Sov. Phys. JETP Lett. 41 (1985) 473.
[59] B.S. Kerner, V.V. Osipov, Sov. Phys. Solid State 21 (1979) 1348.
[60] B.S. Kerner, V.V. Osipov, Sov. Microelectronics 10 (1981) 407.
[61] J. Nagumo, S. Yoshizawa, S. Arimoto, IEEE Trans. Circuit Theory 12 (1965) 400.
[62] J. Rinzel, D. Terman, SIAM J. Appl. Math. 42 (1982) 1111.
[63] R.G. Casten, H. Cohen, A. Lagerstrom, Quart. Appl. Math. 32 (1975) 365.
[64] V.V. Gafiichuk, B.S. Kerner, I.M. Lazurchak, V.V. Osipov, Mikroelektronika 15 (1986) 180 .
[65] V.V. Osipov, V.V. Gafiichuk, B.S. Kerner, I.M. Lazurchak, Mikroelektronika 16 (1987) 23.
[66] V.V. Gafiichuk, V.E. Gashpar, B.S. Kerner, V.V. Osipov, Sov. Phys. Semicond. 22 (1988) 1298.
[67] J.D. Dockery, J.P. Keener, SIAM J. Appl. Math. 49 (1989) 539.
[68] C.B. Muratov, V.V. Osipov, Phys. Rev. E 54 (1996) 4860.
[69] C.B. Muratov, Phys. Rev. E 54 (1996) 3369.
[70] C.B. Muratov, Phys. Rev. E 55 (1997) 1463.
[71] M.N. Vinoslavskii, B.S. Kerner, V.V. Osipov, O.G. Sarbej, J. Phys. Condens. Mater. 2 (1990) 2863.
[72] H. Willebrandt, et al., Phys. Lett. A 149 (1990) 131.
[73] W.N. Reynolds, J.E. Pearson, S. Ponce-Dawson, Phys. Rev. E 56 (1997) 185.
[74] G. Caginalp, P.C. Fife, Phys. Rev. B 33 (1986) 7792.
[75] G. Caginalp, Phys. Rev. A 39 (1989) 5887.
[76] D.W. McLaughlin, D.J. Muraki, M.J. Shelly, Physica D 97 (1996) 471.